

Special
Collection

From Simple Alkenes and CO₂ to Fluorinated Carboxylic Acids: Computational Studies and Predictions

Jorge Echeverría*^[a] and Jesús Jover*^[a]

Fluorinated carboxylic acids may soon become a relevant class of compounds for new materials development and as synthons in medicinal chemistry. In this report, a potential method based on a hydroboration/copper-catalyzed carboxylation reaction sequence has been computationally explored to check whether

these moieties could be synthetically accessible. DFT calculations fully support the possibility of obtaining fluorinated carboxylic acids from simple fluorinated alkenes and gaseous carbon dioxide, paving the way to future preparation of this class of chemicals.

Introduction

Fluorinated carboxylic acids have become relevant synthetic targets because of their potential applications in materials science^[1,2] or as synthons in the preparation of drugs and biologically active precursors (Figure 1).^[3–7] The preparation of fluorinated compounds has largely grown in the last decades due to the key role played by fluorine in medicine.^[8–10] Consequently, many different methods have been developed for introducing functional groups such as CF₃^[11–14] and SCF₃^[15–17] into organic substrates. The addition of these fluorinated functional groups largely enhances the lipophilicity of the resulting product, increasing its ability to travel across cell membranes and boosting its metabolic stability.^[18] On the other hand, the carboxylic acid moiety is a widespread and versatile functional group that can be employed in the preparation of biologically active molecules or as starting point for further functionalization in drug design.^[19–21] Methods for synthesizing fluorinated carboxylic acids are relatively scarce and usually require precious metals or harsh reaction conditions.^[22–27] Therefore, new synthetic strategies leading to the preparation of these compounds will be soon needed.

In recent years, different metal-catalyzed systems have been reported to introduce CO₂ onto organic substrates,^[28–31] often on multiple C–C bonds.^[32–34] One of these systems, reported by Skrydstrup and Nielsen,^[35] was originally devised for hydroboration/carboxylation of disubstituted alkenes and terminal

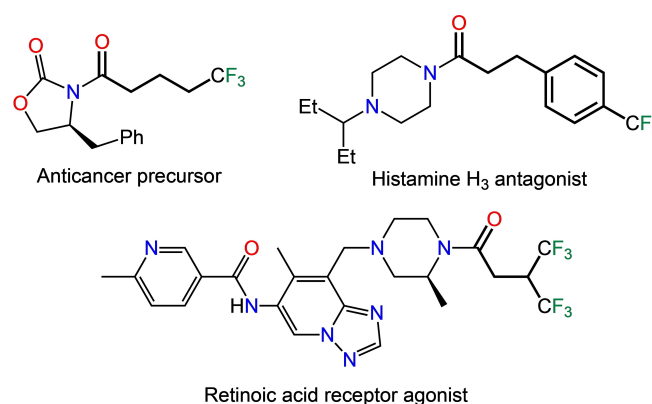
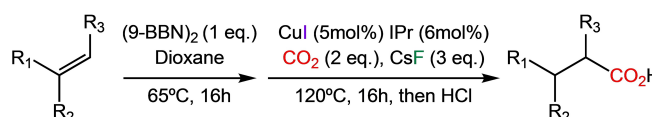


Figure 1. Biologically active molecules prepared from fluorinated carboxylic acids (bold part of the structures).

alkynes but could serve as well for the obtention of fluorinated species relevant to biological and medical applications. Here, by means of a comprehensive computational study, we will explore the performance of this catalytic platform for preparing fluorinated carboxylic acids from small fluorinated alkenes and carbon dioxide.

Results and Discussion

The original reaction of Skrydstrup and Nielsen consists of two independent consecutive steps: 1) hydroboration of the double C–C bond with 9-Borabicyclo[3.3.1]nonane (9-BBN), and 2) copper-catalyzed carboxylation of the resulting borylated product with gaseous CO₂ (Scheme 1). The hydroboration stage should be expected to proceed following the classical con-



Scheme 1. Copper-catalyzed hydroboration/carboxylation of alkenes proposed by Nielsen and Skrydstrup.^[35]

[a] Dr. J. Echeverría, Dr. J. Jover
Secció de Química Inorgànica, Departament de Química Inorgànica i Orgànica & Institut de Química Teòrica i Computacional (IQTC-UB)
Universitat de Barcelona
Martí i Franquès 1–11, 08028, Barcelona, Spain
E-mail: jorge.echeverria@qi.ub.es
jjovermo@ub.edu

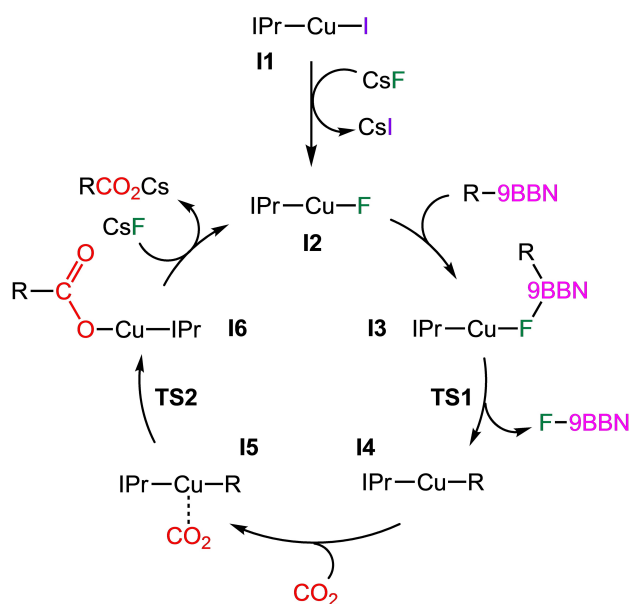
Supporting information for this article is available on the WWW under <https://doi.org/10.1002/ejoc.202101243>

Part of the joint "International Symposium on Homogeneous Catalysis" Special Collection with all Chemistry Europe journals.

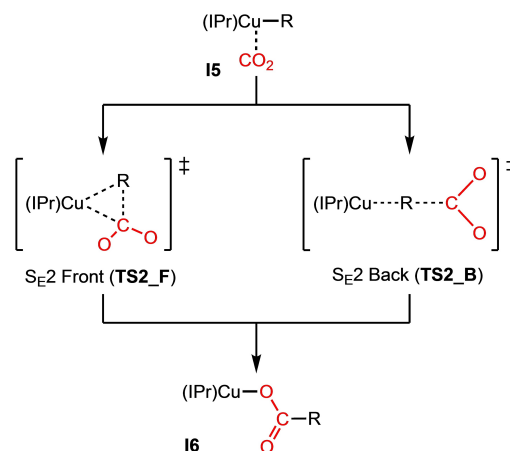
© 2021 The Authors. European Journal of Organic Chemistry published by Wiley-VCH GmbH. This is an open access article under the terms of the Creative Commons Attribution License, which permits use, distribution and reproduction in any medium, provided the original work is properly cited.

certed syn addition mechanism. In the case of having a non-symmetric starting alkene two different products may be formed. Hydroboration of alkenes is known to follow the anti-Markovnikov rule, which states that the boron atom will be placed predominantly on the less substituted carbon of the alkene. In any case, when possible, both hydroboration transition states (Markovnikov and anti-Markovnikov) have been computed for all the substrates.

The general catalytic cycle for the carboxylation reaction is described in Scheme 2. The initial catalyst (**I1**) reacts with CsF to form species **I2**, this is formally an iodide/fluoride replacement, which is usually assumed to proceed smoothly and, thus, the activation energy associated to this step has not been computationally explored. The reaction proceeds by the addition of the borylated substrate to **I2** to deliver complex **I3**. In this compound the fluoride ligand is bound to the boron atom of the incoming substrate. Then the transmetalation step (**TS1**) takes place and the organic moiety replaces the fluoride, producing the copper(I) organometallic intermediate **I4**; consequently, the fluorinated 9-BBN byproduct is released into the reaction mixture. After that, CO₂ comes in, forming a non-covalently bound precursor (**I5**) that evolves into the metal-bound carboxylated product (**I6**) through the corresponding transition state (**TS2**). It must be noted that **TS2** could correspond to front (with configuration retention) or back (with configuration inversion) S_E2-type transition state, **TS2_F** and **TS2_B** in Scheme 3, respectively; these two transition states, which may be both seen as an electrophilic attack of CO₂ onto the copper-coordinated C atom, have been computed in all cases. Finally, the cesium salt of the desired product can be obtained by replacement of the carboxylate with CsF, which takes the catalytic cycle back to species **I2**. The addition of HCl at the end of the reaction furnishes the final carboxylic acid product. A recent report indicates that the carboxylation of



Scheme 2. General catalytic cycle for the copper-catalyzed carboxylation of hydroborated alkenes,



Scheme 3. Possible carboxylation transition states of copper(I) organometallic intermediates.

nonbenzylic substrates requires the copper catalyst, whereas benzylic substrates can be carboxylated both with and without copper using the same catalytic platform.^[36] This pathway has also been computed for selected cases (*vide infra*).

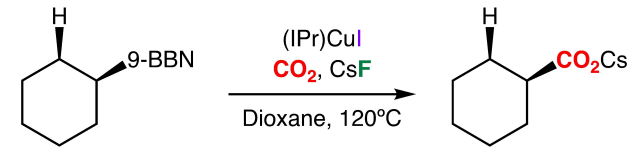
The hydroboration/carboxylation reaction of cyclohexene, one of the originally reported substrates, has been studied before computationally exploring the reaction with fluorinated alkenes. In this way a proper computational methodology could be set and further employed to assess the catalytic activity towards the obtention of fluorinated carboxylic acids. The final methodology (*vide infra*) produces reasonable reaction barriers within a balanced time frame.

The symmetric nature of the double bond of cyclohexene indicates that only one product (9-Cyclohexyl-9-borabicyclo[3.3.1]nonane (Cy-9-BBN)) can be obtained in the hydroboration stage. The transition state barrier associated to this process (28.3 kcal mol⁻¹, at 65 °C) indicates that it should be a quite slow reaction, explaining the relatively long reaction time required. The carboxylation process of Cy-9-BBN (Table 1) takes place following the catalytic cycle shown in Scheme 2. The corresponding computed relative Gibbs energies can be found in Table 1.

As may be observed the overall reaction barrier, located between intermediate **I3** and the front carboxylation transition state **TS2_F**, requires 28.8 kcal mol⁻¹, a reasonable quantity for a reaction running at 120 °C, and similar to the values found in a previous report.^[36] The back-type S_E2 carboxylation transition state (**TS2_B**) is found more than 6 kcal mol⁻¹ higher in energy and can be safely ruled out as a competing process.

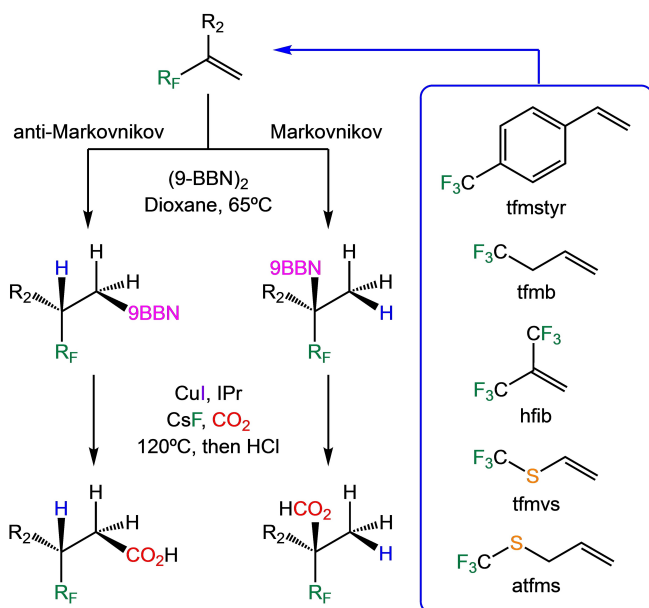
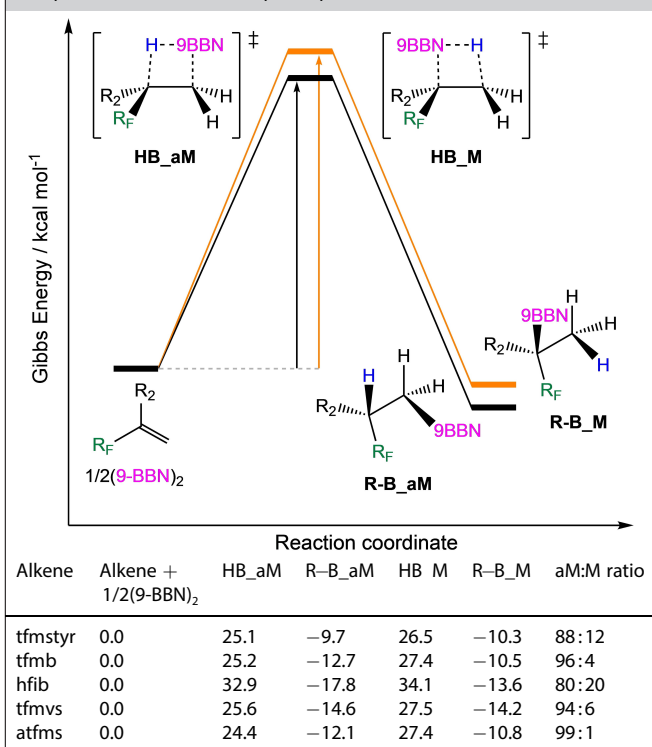
Once a suitable computational methodology has been found, the hydroboration/carboxylation sequence can be computed for five simple fluorinated alkene substrates: 4-(trifluoromethyl)styrene (tfmstyr), 4,4,4-trifluoro-1-butene (tfmb), hexafluoroisobutene (hfib), trifluoromethyl vinyl sulfide (tfmvs) and allyl trifluoromethyl sulfide (atfms) (Scheme 4). Contrary to cyclohexene, these substrates can form different products in the hydroboration stage, coming from either Markovnikov (**M**) or anti-Markovnikov (**aM**) additions. Table 2

Table 1. Copper-catalyzed carboxylation of Cy-9-BBN and computed relative Gibbs energies (in kcal mol⁻¹) for all the species involved in the catalytic cycle.



Step	Relative Gibbs Energy [kcal mol ⁻¹]
I1	0.0
I2	-0.3
I3	-4.5
TS1	22.3
I4	1.9
I5	5.5
TS2_F	24.3
TS2_B	30.5
I6	-16.6
Overall	-23.2
Barrier	28.8

Table 2. Plausible anti-Markovnikov (aM) and Markovnikov (M) hydroboration pathways, relative computed Gibbs energies (in kcal mol⁻¹) for all the species involved and computed product ratios at 65 °C.



Scheme 4. Hydroboration/carboxylation sequence for different starting fluorinated alkenes.

shows the computed Gibbs energies for both hydroboration pathways, in all cases the anti-Markovnikov addition is clearly favored, with barriers *ca.* 1–3 kcal mol⁻¹ lower than their Markovnikov analogues. These values indicate that, at 65 °C, the

anti-Markovnikov product will be preferentially formed for all substrates, see Table 2 for the computed product ratios. In all cases except for hfib the computed anti-Markovnikov hydroboration barriers (HB_aM) are low enough (24.4–25.6 kcal mol⁻¹) to ensure this reaction stage will proceed smoothly under the experimental conditions. Since the anti-Markovnikov products (R-B_aM) are obtained in much larger amounts, only those have been employed as reactants in the computed carboxylation process; although hfib shows a very high hydroboration barrier, it has also been included for completeness.

The computed relative Gibbs energies for the copper-catalyzed carboxylation of the hydroborated fluorinated alkenes can be found in Table 3. As may be observed all the substrates show affordable overall reaction barriers at 120 °C, ranging between 24.5 and 30.2 kcal mol⁻¹.

These barriers correspond always to the carboxylation transition state (TS2). The nature of this transition state is variable: front S_E2 (TS2_F) for tfmb, hfib and atfms, and back S_E2

Table 3. Computed relative Gibbs energies (in kcal mol⁻¹) for all the species involved in the carboxylation catalytic cycle of fluorinated hydroborated alkenes.

Substrate	I1	I2	I3	TS1	I4	I5	TS2_F	TS2_B	I6	Overall	Barrier
tfmstyr	0.0	-0.3	-1.8	12.1	-1.5	2.8	23.5	22.7	-14.3	-21.4	24.5
tfmb	0.0	-0.3	-4.4	13.3	-1.9	3.2	23.1	24.6	-14.5	-23.2	27.6
hfib	0.0	-0.3	-1.7	13.9	-5.5	-1.5	23.4	30.7	-15.7	-23.1	28.9
tfmvs	0.0	-0.3	-6.8	10.2	-4.2	-0.4	24.3	23.4	-14.4	-22.5	30.2
atfms	0.0	-0.3	-4.9	14.4	-3.5	2.6	22.0	25.7	-14.5	-22.8	26.9

(TS2_B) for tfmstyr and tfmvs. However, a clear correlation between the substrate and the structural preference of the transition state could not be clearly envisaged. The larger overall barriers appear for the substrates bearing the fluorinated groups closer to the copper center in intermediate **I4** *i.e.* hfib and tfmvs (28.9 and 30.2 kcal mol⁻¹, respectively) while the lower barrier is found for tfmstyr, where the CF₃ group is placed farther from the metal (24.5 kcal mol⁻¹). This seems to indicate that the carboxylation transition state is strongly influenced by the inductive effects of the fluorinated pending groups, with closer fluorinated substituents hampering the electrophilic attack of CO₂. To explore this effect, the carboxylation barrier, computed as the energy difference between **I4** and TS2_F or TS2_B, has been explored. This barrier takes values of 24.2, 25.0, 28.9, 27.6 and 25.5 kcal mol⁻¹ for tfmstyr, tfmb, hfib, tfmvs and atfms, respectively. First, the possible correlation between the carboxylation barrier and the charge of the carbon atom bound to copper in species **I4** was investigated. None of the computed charges (Mulliken, NBO^[37] and CM5^[38]) show a significant correlation with the barrier and thus, this approximation was discarded.

Next, the Fukui condensed nucleophilic index for the carbon atom bound to copper in **I4** (f_c^-)^[39,40] was computed and correlated with the carboxylation barrier. The f_c^- parameter shows a very good correlation with the barrier ($R^2 = 0.978$) and shows a negative relationship (Barrier = 34.86 - 37.17 f_c^- , Figure 2), indicating that the carbon atoms displaying larger f_c^- , hence with larger nucleophilic character, produce lower carboxylation barriers, as should be expected for an S_E2 reaction such as the one studied here. In contrast, the overall reaction barrier, computed as the energy difference between **I3** and TS2 for all substrates except for hfib, cannot be correlated with any of the computed charges or the Fukui reactivity indexes.

The alternative copper-free CsF-catalyzed carboxylation reaction, as proposed by Hopmann et al.,^[36] has been computed

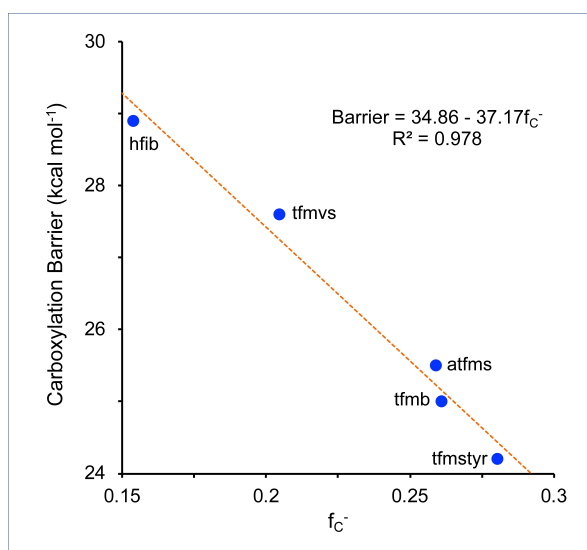


Figure 2. Linear correlation between the f_c^- index and the carboxylation barrier for fluorinated alkene substrates.

for tfmstyr and atfms. In agreement with their results, these two nonbenzylic substrates show a much higher transmetalation barrier than their copper-catalyzed counterparts: 46.1 and 40.1 kcal mol⁻¹ for tfmstyr and atfms, respectively, consequently ruling out the CsF-catalyzed pathway. Given the nonbenzylic nature of the remaining fluorinated alkene substrates, this pathway has not been further explored.

Conclusion

This computational exploration clearly indicates that the synthesis of fluorinated carboxylic acids from simple alkenes and carbon dioxide could be easily achievable with the studied catalytic platform. Both the hydroboration and the copper-catalyzed carboxylation stages present affordable reaction barriers under the experimental reaction conditions. Experimental corroboration of the proposed synthetic process is currently underway and will be reported in due course.

Experimental Section

All the structures have been fully optimized in 1,4-dioxane (in PCM, see below) using the Gaussian09^[41] suite of programs with the B3LYP^[42-45] functional. In the optimization process the TZVP basis set of Ahlrichs^[46,47] was used for all atoms except for Cs, for which the Def2-SVPD basis set,^[48] along with the corresponding pseudo-potential, was employed. Ultrafine integration grids have been used to ensure satisfactory convergence. This is necessary because some of the species under study present a number of low frequency vibrational modes (< 100 cm⁻¹) that contribute significantly to the entropy and have to be computed properly. In all cases the solvation energies in 1,4-dioxane are computed with the (IEF-PCM)^[49,50] continuum dielectric solvation model using the SMD^[51] radii and non-electrostatic terms. The dispersion correction terms have been included by using the D3 method of Grimme^[52] with the Becke-Jonhson damping parameter set to zero. These computational settings are named BS1. In all cases frequency calculations are carried out to ensure the nature of stationary points and transition states. Additional single point calculations, including solvation and dispersion corrections, on the optimized geometries are employed to obtain improved Gibbs energy values with larger basis sets (BS2). In these calculations, the B3LYP functional was kept and the Def2-TZVPPD basis set^[48] was employed to describe all atoms.

The computed Gibbs energies were corrected to use a standard state corresponding to species in solution with a standard concentration of 1 M. The final Gibbs energies at a given temperature, computed based on the rigid rotor/harmonic oscillator approach to statistical mechanics, are obtained with the following formula:

$$G_T^\circ = E_{BS2} + H_{corr,BS1} - TS_{BS1} + RT \ln(C^\circ / C_{1atm})$$

where E_{BS2} is the electronic energy, including the solvent and dispersion terms, obtained with the large basis sets (BS2). $H_{corr,BS1}$ is the thermal correction to enthalpy and contains the zero-point energy plus the vibrational, rotational and translational energies. Finally, TS_{BS1} accounts for the entropic correction. Both these terms are obtained with the small basis sets (BS1). Gibbs energies as output by Gaussian, which refer to an ideal gas ($P = 1$ atm) standard

state, were corrected to use a standard state corresponding to species in solution with a standard concentration of 1 M. This was performed by adding an extra term to the Gaussian computed Gibbs energy of each species; this correction is computed as $RT \ln(C^\circ/C_{1atm})$, where C° is the standard reference state concentration (1 M), and C_{1atm} is the concentration of an ideal gas under the standard $P=1$ atm conditions ($C_{1atm}=1/V_m=P/RT=0.036$ and 0.0310 M for an ideal gas at 1 atm and at 338.15 and 393.15 K, respectively). Numerically, these corrective terms equal to 2.23 and $2.71 \text{ kcal mol}^{-1}$ per molecule at 338.15 and 393.15 K, respectively.

The Fukui nucleophilicity index for the carbon atom bound to copper in species **14** (f_c^-) has been computed from the NBO^[37] populations obtained in single point calculations employing the B52 computational settings. This index indicates the tendency of the carbon atom to behave as a nucleophile in a given reaction and is computed as: $f_c^- = P_c(N) - P_c(N-1)$,^[39,40] where $P_c(N)$ stands for the population of the C atom bound to copper in **14** and $P_c(N-1)$ is the population of the same C atom in the monovalent cationic species of **14** i.e. **14** minus one electron.

Given the computational nature of this study, and to assess the validity of the methodology employed, the overall reaction barrier of the Cy-9-BBN substrate has been computed with different functionals displaying variable HF amounts, namely PBE,^[53,54] M06^[55] and M062X.^[55] A single point calculation for all the species involved (**13**, **TS2_F**, F-9-BBN and CO_2) with these functionals and the B52 settings has been performed while the vibrational and enthalpic corrections with B3LYP functionals along with the rest of B51 settings were kept. The computed barriers are 20.6, 28.8, 29.9 and $32.6 \text{ kcal mol}^{-1}$ for PBE, B3LYP, M06 and M062X, respectively. These results suggest that the reaction has a relatively strong ionic character and changing the HF amount of the functional affects the barrier height (higher HF percentage produces a higher barrier). These calculations, by themselves, do not shed light on the validity of the B3LYP functional to model the reaction and therefore, a reduced kinetic modeling of the process has been carried out. Using the B3LYP functional, the carboxylation of Cy-9-BBN is computed to have an overall barrier of $28.8 \text{ kcal mol}^{-1}$. This barrier, when transformed into a rate constant with the Eyring-Polanyi equation for a bimolecular reaction such as the one determining the rate-limiting step: $\text{13} + \text{CO}_2 \rightarrow \text{16} + \text{F-9-BBN}$, produces a value of $k = 8.5 \cdot 10^{-4} \text{ M}^{-1} \text{ s}^{-1}$, which falls in the adequate range for a reaction operating at 120°C : 98% simulated yield in 16 hours. Among the rest of the functionals tested, an alternative could be M06, which provides a barrier ($29.9 \text{ kcal mol}^{-1}$) close to that of B3LYP. On the other hand, PBE produces a too low ($20.6 \text{ kcal mol}^{-1}$) overall barrier whereas M062X seems to provide a too high energy barrier ($32.6 \text{ kcal mol}^{-1}$).

Acknowledgements

J. E. is grateful to the Spanish MICCIN for a Ramón y Cajal contract (RYC-2017-22853) and a Generación de Conocimiento research project (PID2019-109119GA-I00). Additional financial support from MINECO (PGC2018-093863-B-C21) and the Spanish Structures of Excellence María de Maeztu program (MDM-2017-0767) is gratefully acknowledged.

Conflict of Interest

The authors declare no conflict of interest.

Keywords: Carbon dioxide fixation · Carboxylation · Density functional calculations · Homogeneous catalysis · Hydroboration

- [1] H. Pinfold, C. Greenland, G. Pattison, G. Costantini, *Chem. Commun.* **2020**, 56, 125–128.
- [2] A. A. Rand, S. A. Mabury, *Environ. Sci. Technol.* **2011**, 45, 8053–8059.
- [3] F. Zaragoza, H. Stephensen, S. M. Knudsen, L. Pridal, B. S. Wulff, K. Rimvall, *J. Med. Chem.* **2004**, 47, 2833–2838.
- [4] F. Lehmann, L. Lake, E. A. Currier, R. Olsson, U. Hacksell, K. Luthman, *Eur. J. Med. Chem.* **2007**, 42, 276–285.
- [5] M. Flipo, M. Desroses, N. Lecat-Guillet, B. Villemagne, N. Blondiaux, F. Leroux, C. Piveteau, V. Mathys, M.-P. Flament, J. Siepmann, V. Villeret, A. Wohlkönig, R. Wintjens, S. H. Soror, T. Christophe, H. K. Jeon, C. Lochet, P. Brodin, B. Déprez, A. R. Baulard, N. Willand, *J. Med. Chem.* **2012**, 55, 68–83.
- [6] A. V. Gavai, C. Quesnelle, D. Norris, W.-C. Han, P. Gill, W. Shan, A. Balog, K. Chen, A. Tebben, R. Rampulla, D.-R. Wu, Y. Zhang, A. Mathur, R. White, A. Rose, H. Wang, Z. Yang, A. Ranasinghe, C. D'Arienzo, V. Guarino, L. Xiao, C. Su, G. Everlof, V. Arora, D. R. Shen, M. E. Cvijic, K. Menard, M.-L. Wen, J. Meredith, G. Trainor, L. J. Lombardo, R. Olson, P. S. Baran, J. T. Hunt, G. D. Vite, B. S. Fischer, R. A. Westhouse, F. Y. Lee, *ACS Med. Chem. Lett.* **2015**, 6, 523–527.
- [7] R. Nakajima, H. Oono, S. Sugiyama, Y. Matsueda, T. Ida, S. Kakuda, J. Hirata, A. Baba, A. Makino, R. Matsuyama, R. D. White, R. P. Wurz, Y. Shin, X. Min, A. Guzman-Perez, Z. Wang, A. Symons, S. K. Singh, S. R. Mothe, S. Belyakov, A. Chakrabarti, S. Shuto, *ACS Med. Chem. Lett.* **2020**, 11, 528–534.
- [8] K. Müller, C. Faeh, F. Diederich, *Science* **2007**, 317, 1881–1886.
- [9] S. Purser, P. R. Moore, S. Swallow, V. Gouverneur, *Chem. Soc. Rev.* **2008**, 37, 320–330.
- [10] T. Scattolin, S. Bouayad-Gervais, F. Schoenebeck, *Nature* **2019**, 573, 102–107.
- [11] O. A. Tomashenko, V. V. Grushin, *Chem. Rev.* **2011**, 111, 4475–4521.
- [12] T. Furuya, A. S. Kamlet, T. Ritter, *Nature* **2011**, 473, 470–477.
- [13] J. Jover, *ACS Catal.* **2014**, 4, 4389–4397.
- [14] G. Li, C. Zhang, C. Song, Y. Ma, *Beilstein J. Org. Chem.* **2018**, 14, 155–181.
- [15] X.-H. Xu, K. Matsuzaki, N. Shibata, *Chem. Rev.* **2015**, 115, 731–764.
- [16] M. A. Hardy, H. Chachignon, D. Cahard, *Asian J. Org. Chem.* **2019**, 8, 591–609.
- [17] J. Jover, *Catal. Sci. Technol.* **2019**, 9, 5962–5970.
- [18] A. Leo, C. Hansch, D. Elkins, *Chem. Rev.* **1971**, 71, 525–616.
- [19] P. J. Hajduk, M. Bures, J. Praestgaard, S. W. Fesik, *J. Med. Chem.* **2000**, 43, 3443–3447.
- [20] C. Lamberth, J. Dinges, in *Bioact. Carboxylic Compd. Classes*, **2016**, pp. 1–11.
- [21] Y. Lou, J. Zhu, in *Bioact. Carboxylic Compd. Classes*, **2016**, pp. 221–236.
- [22] J. Lazar, W. A. Sheppard, *J. Med. Chem.* **1968**, 11, 138–140.
- [23] M. Van Der Puy, A. J. Poss, P. J. Persichini, L. A. S. Ellis, *J. Fluorine Chem.* **1994**, 67, 215–224.
- [24] A. Alkayal, V. Tabas, S. Montanaro, I. A. Wright, A. V. Malkov, B. R. Buckley, *J. Am. Chem. Soc.* **2020**, 142, 1780–1785.
- [25] A. Gevorgyan, K. H. Hopmann, A. Bayer, *ChemSusChem* **2020**, 13, 2080–2088.
- [26] J.-J. Ma, W.-B. Yi, G.-P. Lu, C. Cai, *Catal. Sci. Technol.* **2016**, 6, 417–421.
- [27] G. Choi, G. S. Lee, B. Park, D. Kim, S. H. Hong, *Angew. Chem. Int. Ed.* **2021**, 60, 5467–5474; *Angew. Chem.* **2021**, 133, 5527–5534.
- [28] B. Chan, Y. Luo, M. Kimura, *Aust. J. Chem.* **2018**, 71, 272–278.
- [29] Y. Mori, C. Shigeno, Y. Luo, B. Chan, G. Onodera, M. Kimura, *Synlett* **2018**, 29, 742–746.
- [30] Y. Luo, B. Chan, T. Fukuda, G. Onodera, M. Kimura, *Synlett* **2021**, 32, 1551–1554.
- [31] N. N. Baughman, N. G. Akhmedov, J. L. Petersen, B. V. Popp, *Organometallics* **2021**, 40, 23–37.
- [32] T. Ohishi, L. Zhang, M. Nishiura, Z. Hou, *Angew. Chem. Int. Ed.* **2011**, 50, 8114–8117; *Angew. Chem.* **2011**, 123, 8264–8267.
- [33] H. Ohmiya, M. Tanabe, M. Sawamura, *Org. Lett.* **2011**, 13, 1086–1088.
- [34] J. Jover, F. Maseras, *J. Org. Chem.* **2014**, 79, 11981–11987.
- [35] M. Juhl, S. L. R. Laursen, Y. Huang, D. U. Nielsen, K. Daasbjerg, T. Skrydstrup, *ACS Catal.* **2017**, 7, 1392–1396.
- [36] M. F. Obst, A. Gevorgyan, A. Bayer, K. H. Hopmann, *Organometallics* **2020**, 39, 1545–1552.

- [37] E. D. Glendening, J. K. Badenhop, A. D. Reed, J. E. Carpenter, F. Weinhold, *NBO 3.1, Theor. Chem. Institute, Univ. Wisconsin-Madison, WI*, **1996**.
- [38] A. V. Marenich, S. V. Jerome, C. J. Cramer, D. G. Truhlar, *J. Chem. Theory Comput.* **2012**, *8*, 527–541.
- [39] P. Bultinck, R. Carbó-Dorca, W. Langenaeker, *J. Chem. Phys.* **2003**, *118*, 4349–4356.
- [40] J. Melin, P. W. Ayers, J. V. Ortiz, *J. Phys. Chem. A* **2007**, *111*, 10017–10019.
- [41] M. J. Frisch, G. W. Trucks, H. B. Schlegel, G. E. Scuseria, M. A. Robb, J. R. Cheeseman, G. Scalmani, V. Barone, B. Mennucci, G. A. Petersson, H. Nakatsuji, M. Caricato, X. Li, H. P. Hratchian, A. F. Izmaylov, J. Bloino, G. Zheng, J. L. Sonnenberg, M. Hada, M. Ehara, K. Toyota, R. Fukuda, J. Hasegawa, M. Ishida, T. Nakajima, Y. Honda, O. Kitao, H. Nakai, T. Vreven, J. A. Montgomery Jr., J. E. Peralta, F. Ogliaro, M. Bearpark, J. J. Heyd, E. Brothers, K. N. Kudin, V. N. Staroverov, R. Kobayashi, J. Normand, K. Raghavachari, A. Rendell, J. C. Burant, S. S. Iyengar, J. Tomasi, M. Cossi, N. Rega, J. M. Millam, M. Klene, J. E. Knox, J. B. Cross, V. Bakken, C. Adamo, J. Jaramillo, R. Gomperts, R. E. Stratmann, O. Yazyev, A. J. Austin, R. Cammi, C. Pomelli, J. W. Ochterski, R. L. Martin, K. Morokuma, V. G. Zakrzewski, G. A. Voth, P. Salvador, J. J. Dannenberg, S. Dapprich, A. D. Daniels, O. Farkas, J. B. Foresman, J. V. Ortiz, J. Cioslowski, D. J. Fox, *Gaussian 09, Revision D.01, Gaussian, Inc., Wallingford CT*, **2013**.
- [42] S. H. Vosko, L. Wilk, M. Nusair, *Can. J. Phys.* **1980**, *58*, 1200–1211.
- [43] C. Lee, W. Yang, R. G. Parr, *Phys. Rev. B* **1988**, *37*, 785–789.
- [44] A. D. Becke, *J. Chem. Phys.* **1993**, *98*, 5648–5652.
- [45] P. J. Stephens, F. J. Devlin, C. F. Chabalowski, M. J. Frisch, *J. Phys. Chem.* **1994**, *98*, 11623–11627.
- [46] A. Schäfer, H. Horn, R. Ahlrichs, *J. Chem. Phys.* **1992**, *97*, 2571–2577.
- [47] A. Schäfer, C. Huber, R. Ahlrichs, *J. Chem. Phys.* **1994**, *100*, 5829.
- [48] F. Weigend, R. Ahlrichs, *Phys. Chem. Chem. Phys.* **2005**, *7*, 3297–3305.
- [49] J. Tomasi, B. Mennucci, R. Cammi, *Chem. Rev.* **2005**, *105*, 2999–3094.
- [50] G. Scalmani, M. J. Frisch, *J. Chem. Phys.* **2010**, *132*, 114110.
- [51] A. V. Marenich, C. J. Cramer, D. G. Truhlar, *J. Phys. Chem. B* **2009**, *113*, 6378–6396.
- [52] S. Grimme, S. Ehrlich, L. Goerigk, *J. Comput. Chem.* **2011**, *32*, 1456–1465.
- [53] J. Perdew, K. Burke, M. Ernzerhof, *Phys. Rev. Lett.* **1996**, *77*, 3865–3868.
- [54] J. P. Perdew, K. Burke, M. Ernzerhof, *Phys. Rev. Lett.* **1997**, *78*, 1396.
- [55] Y. Zhao, D. G. Truhlar, *Theor. Chem. Acc.* **2008**, *120*, 215–241.

Manuscript received: October 7, 2021
Revised manuscript received: November 19, 2021
Accepted manuscript online: November 23, 2021